J Inorg Organomet Polym (2012) 22:1325–1331
DOI 10.1007/s10904-012-9760-2

Synthesis, Crystal Structure, Spectroscopic and Thermal Investigations of a Novel 2D Sodium(I) Coordination Polymer Based on 2-Aminoterephthalic Ligand

Justyna Sienkiewicz-Gromiuk · Liliana Mazur · Agata Bartyzel · Zofia Rzączyńska

Received: 6 July 2012 / Accepted: 10 September 2012 / Published online: 28 September 2012

Abstract The reaction of sodium hydroxide with 2-aminoterephthalic acid leads to the formation of a complex of the general formula: $[Na_2(atpt)(H_2O)_5]\cdot H_2O$, where atpt = $[NH_2C_6H_3(COO)_2]^{2-}$. Sodium 2-aminoterephthalate was synthesized and characterized by single-crystal X-ray diffraction, FT-IR spectroscopy, thermal analysis and coupled TG–FT-IR technique. Crystallographic study of the sodium complex reveals that the compound crystallizes in the triclinic system, the space group *P*-1 with $a = 7.983(3)$ Å, $b = 8.405(3)$ Å, $c = 11.311(5)$ Å, $\alpha = 70.74(3)°$, $\beta = 76.57(3)°$, $\gamma = 83.12(3)°$ and $V = 696.1(5)$ Å^3. On heating in air atmosphere the compound in question loses all water molecules in two steps in the temperature range 30–205 °C. The anhydrous form of the complex is stable up to 370 °C and then decomposes to sodium carbonate.

Keywords 2-Aminoterephthalic acid · Sodium(I) complex · Coordination polymer · Crystal structure · Thermal studies

1 Introduction

In recent years the design and synthesis of coordination polymers has undergone explosive growth (in supramolecular and materials chemistry) due to the variety of interesting structural topologies, physico-chemical properties and potential applications as functional materials [1–3]. Coordination polymers formed on the basis of metal ions tethered by rigid, functional organic linkers constitute a wide group of porous compounds named MOFs (metal–organic frameworks) [4, 5]. The architectures of polymeric networks are delineated by crystalline structure, which can be self-assembled by the coordination of metal ions with multidentate organic linkers containing O and/or N donors [6–10]. The presence of O and N donor atoms in the ligand molecules enables formation of hydrogen bonds, which can interlink 1D or 2D structures into higher dimensional systems. Furthermore, the supramolecular architectures are exploited by aromatic π–π stacking interactions, electrostatic and charge-transfer attractions [11–14].

Recently much attention has been paid to study metal complexes containing benzenedicarboxylate anions, because such ligands display several different coordination modes. 2-Aminoterephthalic acid ($H_2atpt = NH_2C_6H_3(COOH)_2$) as a derivative of 1,4-benzenedicarboxylic acid is a good organic building block for construction of extended open frameworks. The structural formula of the neutral H_2atpt is shown in Scheme 1. In fact, many studies about atpt were focused on lanthanide and transition metal coordination polymers [15–24]. In the structure of these complexes only carboxylate groups of atpt ligand take part in metal bonding. The substituted amino group does not coordinate metal centers even so it may act as a proton acceptor or donor in many hydrogen bonds and affects the coordination mode of the carboxylic groups [15–18]. However, alkali-metal complexes with the atpt ligand have not been reported. Herein, we report the synthesis, crystal structure and thermal behaviour of the novel coordination polymer named $[Na_2(atpt)(H_2O)_5]\cdot H_2O$, where atpt = $[NH_2C_6H_3(COO)_2]^{2-}$.

J. Sienkiewicz-Gromiuk · L. Mazur · A. Bartyzel · Z. Rzączyńska (✉)
Department of General and Coordination Chemistry, Faculty of Chemistry, Maria Curie-Skłodowska University, M. Curie-Skłodowska Sq. 2, 20-031 Lublin, Poland
e-mail: z.rzaczynska@poczta.umcs.lublin.pl

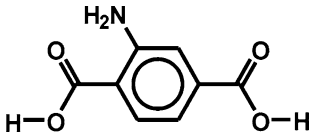

Scheme 1 The structural formula of the neutral H_2atpt (2-aminoterephthalic acid)

2 Experimental Methods

2.1 Materials

2-Aminoterephthalic acid (99 %) was purchased from ALDRICH Inc. Sodium hydroxide (99.99 %) was purchased from POCH S.A. All the chemicals were used without any further purification.

2.2 Synthesis of $[Na_2(atpt)(H_2O)_5]\cdot H_2O$

A hot solution of sodium hydroxide (0.16 g, 4.0 mmol) in 10 mL of water was combined with 2-aminoterephthalic acid (0.36 g, 2.0 mmol) in 5 mL of water. The mixture of solution of sodium hydroxide and the water suspension of 2-aminoterephthalic acid was heated in the aqueous bath at 45 °C for 1 h. The light yellowish solution was filtered. Transparent crystals tinged with beige, suitable for the single-crystal X-ray analysis were obtained by slow evaporation of an aqueous solution after a few weeks. The changes in the synthesis conditions, like different metal-to-ligand ratio or solvent media, do not influence the structure and composition of the final product. Anal. Calcd. for $C_8H_{17}NO_{10}Na_2$ (333.15): C 28.816, H 5.103, N 4.202 %; found: C 28.725, H 5.041, N 4.176 %. FT-IR data (KBr) ν: 3436, 3393, 3280, 1573, 1371, 427 cm^{-1}.

2.3 Physical Measurements

Elemental analysis was made to determine the content of carbon, hydrogen and nitrogen in the analyzed compound using a CHN 2400 Perkin Elmer analyzer.

Single-crystal diffraction data were measured at room temperature by means of the Oxford Diffraction Xcalibur diffractometer using graphite-monochromated Mo Kα radiation ($\lambda = 0.71073$ Å). The crystallographic data and the refinement procedure details are given in Table 1. All data were corrected for Lorentz, polarization and absorption effects. Crystal structure was solved by direct methods (program SHELXS97) and refined by the full-matrix least-squares method for all F^2 data using the SHELXL97 [25] programs. All non-hydrogen atoms were refined with anisotropic displacement parameters. Hydrogen atoms were located from the difference Fourier map and not refined. The selected geometric parameters are listed in Table 2.

Table 1 Crystal data and structure refinement details for $[Na_2(atpt)(H_2O)_5]\cdot H_2O$

	$[Na_2(atpt)(H_2O)_5]\cdot H_2O$
Empirical formula	$C_8H_{17}NO_{10}Na_2$
Formula weight	333.21
Temperature, [K]	295(2)
Wavelength, [Å]	0.71073
Crystal system	Triclinic
Space group	*P*-1
Unit cell dimensions	
a, [Å]	7.983(3)
b, [Å]	8.405(3)
c, [Å]	11.311(5)
α, [°]	70.74(3)
β, [°]	76.57(3)
γ, [°]	83.12(3)
Volume, [$Å^3$]	696.1(5)
Z	2
Calculated density, [g cm^{-3}]	1.590
Absorption coefficient, [mm^{-1}]	0.195
F (000)	348
Crystal size, [mm]	0.40 × 0.30 × 0.15
θ range for data collection, [°]	3.59–30.07
Unique reflections (R_{int})	4,065 (0.0314)
Goodness-of-fit on F^2	1
Final R indices [$I > 2\sigma(I)$]	$R_1 = 0.0458$; $wR_2 = 0.0984$
R indices (all data)	$R_1 = 0.1255$; $wR_2 = 0.1216$
Largest diff. peak and hole, [e $Å^{-3}$]	0.35 and −0.27

$R_1 = \sum||F_o| - |F_c||/\sum|F_o|$

$wR_2 = \{\sum[w(F_o^2-F_c^2)]^2/\sum[w(F_o^2)]^2\}^{1/2}$

The FT-IR spectrum of the complex was recorded over the range 4,000–400 cm^{-1} using a spectrometer FTIR 1725X Perkin Elmer. The samples were prepared as KBr discs.

Thermal analysis of the prepared complex in air was performed by the TG–DTA method using the Setsys 16/18 apparatus. The sample (8 mg) was heated in the Al_2O_3 crucible at 30–750 °C in flowing air atmosphere with a heating rate of 5 °C min^{-1}. Products of decomposition were calculated from the TG curve.

Gaseous products of decomposition were identified by means of the TG–FT-IR coupled technique using a Netzsch TG apparatus coupled with a Bruker FT-IR IFS66 spectrophotometer. The sample was heated to 750 °C with a Netzsch DSC 204, using the Al_2O_3 crucible, in dynamic argon atmosphere at a heating rate of 10 °C min^{-1}.

Table 2 Selected bond lengths [Å] and angles [°] for $[Na_2(atpt)(H_2O)_5]\cdot H_2O$

Bond lengths [Å]			
Na1–O1w	2.505(2)	Na2–O1w	2.326(2)
Na1–O2w	2.493(2)	Na2–O2w	2.418(2)
Na1–O3w	2.372(2)	Na2–O5w	2.336(2)
Na1–O3w$^{(ii)}$	2.422(2)	Na2–O1	2.373(2)
Na1–O4w	2.468(2)	Na2–O2	2.919(2)
Na1–O4$^{(i)}$	2.376(2)	Na2–O2$^{(iii)}$	2.325(2)
C1k–O1	1.264(2)	C2k–O3	1.267(2)
C1k–O2	1.254(2)	C2k–O4	1.245(2)
Bond angles [°]			
O2w–Na1–O1w	85.0(1)	O1w–Na2–O1	92.1(1)
O3w–Na1–O4w	88.6(1)	O5w–Na2–O1	84.8(1)
O4w–Na1–O2w	98.9(1)	O1–Na2–O2w	102.2(1)
O3w–Na1–O1w	83.6(1)	O1w–Na2–O2w	90.7(1)
O4w–Na1–O1w	81.5(1)	O5w–Na2–O2w	96.8(1)
O3w–Na1–O3w$^{(ii)}$	86.0(1)	O5w–Na2–O2	67.3(1)
O4$^{(i)}$–Na1–O3w$^{(ii)}$	85.6(1)	O1w–Na2–O2	105.6(1)
O3w–Na1–O4$^{(i)}$	88.0(1)	O2$^{(iii)}$–Na2–O2	94.6(1)
O3w$^{(ii)}$–Na1–O2w	82.6(1)	O2$^{(iii)}$–Na2–O1w	87.7(1)
O3w$^{(ii)}$–Na1–O1w	77.6(1)	O2$^{(iii)}$–Na2–O5w	90.2(1)
O4$^{(i)}$–Na1–O4w	114.7(1)	O1–Na2–O2	47.9(1)
O3w$^{(ii)}$–Na1–O4w	158.8(1)	O2w–Na2–O2	145.3(1)
O3w–Na1–O2w	165.3(1)	O1w–Na2–O5w	172.3(1)
O4$^{(i)}$–Na1–O2w	100.2(1)	O2$^{(iii)}$–Na2–O1	140.8(1)
O4$^{(i)}$–Na1–O1w	161.7(1)	O2$^{(iii)}$–Na2–O2w	117.0(1)
O2–C1k–O1	122.4(2)	O4–C2k–O3	124.2(2)

Symmetry codes: (i) x, $y-1$, $z+1$; (ii) $-x+1$, $-y+2$, $-z+1$; (iii) $-x$, $-y+3$, $-z+1$

3 Results and Discussion

3.1 Description of the Crystal Structure of $[Na_2(atpt)(H_2O)_5]\cdot H_2O$

Single-crystal X-ray diffraction study of sodium complex reveals that there are two crystallographically unique Na(I) centers in the structure, though both Na1 and Na2 are six-coordinate (Fig. 1). The coordination environment of Na1 is formed by five oxygen atoms from the water molecules and still another from the carboxylate group. Na2 ion is ligated by three oxygen atoms of water molecules and three oxygen atoms of carboxylate groups. The Na–O_{aqua} distances vary in the range 2.326(2)–2.505(2) Å whereas the Na–$O_{carboxyl}$ bond lengths generally range from 2.325(2) to 2.376(2) Å. However, one longer distance occurs (Na2–O2 = 2.919(2) Å), indicating nonsymmetrical chelation of the carboxylate (O1–C1k–O2) group to Na2. The same effect was previously observed for other NaO_2CR structures with the polydentate bridging-chelating carboxylate groups [26]. Large differences in bond lengths cause significant distortion of coordination polyhedra. Nevertheless, the coordination geometry around the sodium ions can be best described as distorted octahedra. The adjacent Na1 and Na2 ions in the analyzed complex are connected via two water molecules to form a dinuclear building block. Centrosymmetric, head-to-head oriented blocks are further bridged by two atpt ligands to form tetranuclear $Na_4(atpt)_2(H_2O)_{10}$ subunits which are interconnected through other water molecules and the atpt ligands to form 2D layers parallel to (111) plane (Fig. 2a). The distances between Na ions within the layer are 3.485(2) Å for Na1…Na2, 3.585(2) Å for Na2…Na2$^{(i)}$ (symmetry codes as in Table 2) and 3.507(2) Å for Na1…Na1$^{(iii)}$. The hydrogen-bonding arrays extend the 2D layer structure into the 3D supramolecular architecture through interactions between the coordination and lattice water molecules as well as O atoms of carboxylate groups and amine N atoms (Fig. 2b). The complete list of hydrogen bonds and their geometric parameters are given in Table 3.

The geometric parameters of both carboxylic groups are not significantly affected by their coordination modes. The C–O distances in both $–COO^-$ systems are almost the same, in the range of 1.245(2)–1.267(2) Å, which confirms deprotonation of both carboxylic groups. The O–C–O bond angles are 122.4(2)° and 124.2(2)° for the tridentate bridging-chelating and monodentate groups respectively and they form dihedral angles of 13.2(3)° and 23.8(3)° with the phenyl ring plane. Interestingly, the amine nitrogen atom does not participate in coordination. To the best of our knowledge, the coordination mode of 2-aminoterephthalate in the analyzed sodium complex has not been observed in any other coordination polymer containing this ligand [27].

3.2 FT-IR Spectroscopy

The vibrational frequencies obtained from the FT-IR spectra of sodium 2-aminoterephthalate was compared with that came from the spectra of free 2-aminoterephthalic acid (Table 4). In the experimental spectrum of H_2atpt acid, the characteristic frequencies are given on the basis of previously reported study concerning the vibrational spectrum of this compound in the KBr matrix [28]. The most characteristic band at 1,686 cm^{-1} corresponds to the stretching vibrations of C=O of the carboxylic groups, whereas the two sharp bands at 3,507 and 3,393 cm^{-1} were assigned to the stretching asymmetric vibrations of the NH_2 group.

During complex formation the band at 1,690 cm^{-1} corresponding to the C=O stretching vibrations of carboxylic group disappears. At the same time, in the

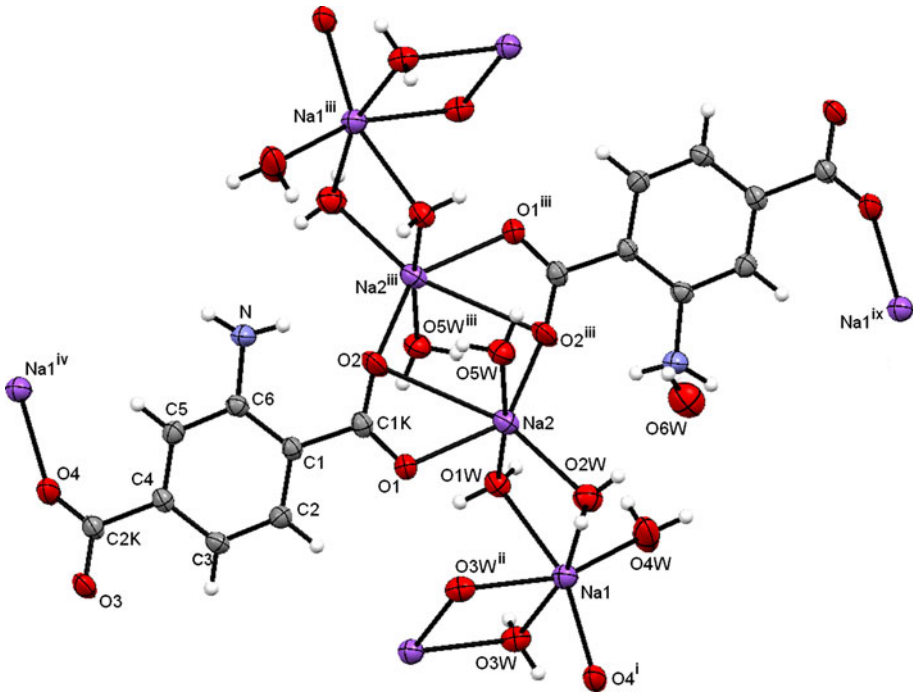

Fig. 1 The molecular structure of title complex with the atom labeling scheme. Symmetry codes: (i) x, y−1, z + 1; (ii) −x + 1, −y + 2, −z + 1; (iii) −x, −y + 3, −z + 1; (iv) x, y + 1, z−1; (ix) −x, −y + 2, −z + 2

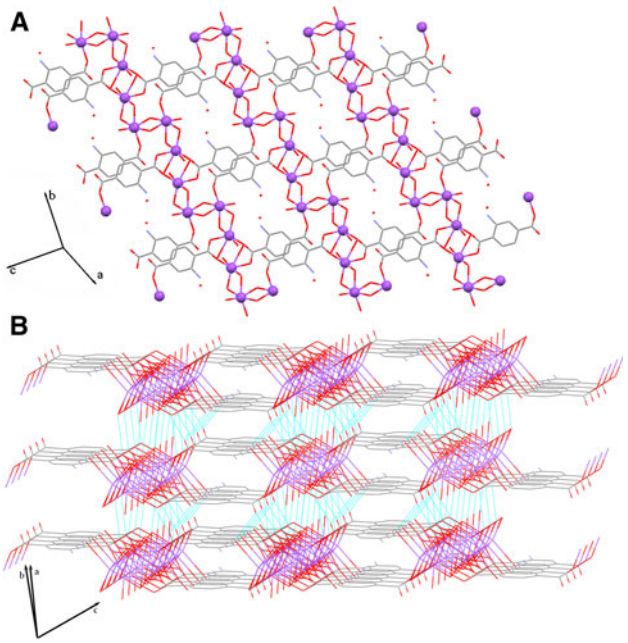

Fig. 2 **a** 2D structure of sodium 2-aminoterephthalate. Hydrogen atoms have been omitted for clarity, **b** hydrogen-bonding interactions between layers (*dotted lines*). Uncoordinated water molecules and all hydrogen atoms have been omitted

Table 3 Hydrogen-bonding geometry [Å, °] for $[Na_2(atpt)(H_2O)_5]\cdot H_2O$

D–H…A	D–H	H…A	D…A	∠DH…A
O5w–H2w5…O2	0.80	2.29	2.950(3)	140
N–H2n…O2	0.88	2.02	2.710(3)	134
O1w–H1w1…O3$^{(v)}$	0.87	2.01	2.860(2)	165
O1w–H2w1…O4$^{(vi)}$	0.89	1.90	2.777(2)	171
O2w–H1w2…O6w	0.80	2.11	2.889(3)	166
O2w–H2w2…O1$^{(vii)}$	0.88	1.95	2.817(2)	166
O3w–H1w3…O5w$^{(viii)}$	0.85	1.96	2.793(2)	167
O3w–H2w3…O1$^{(ii)}$	0.84	1.97	2.792(2)	167
O4w–H1w4…O6w$^{(ix)}$	0.88	2.06	2.915(3)	166
O4w–H2w4…O3$^{(v)}$	0.93	1.84	2.765(3)	169
O5w–H1w5…O3$^{(x)}$	0.82	1.95	2.738(2)	163
O6w–H1w6…O4w$^{(xi)}$	0.91	2.25	3.132(3)	161
O6w–H2w6…N$^{(iii)}$	0.96	1.85	2.813(3)	176
N–H1n…O6w$^{(iv)}$	0.95	2.50	3.353(3)	150

Symmetry codes: (ii) $-x + 1, -y + 2, -z + 1$; (iii) $-x, -y + 3, -z + 1$; (iv) $x, y + 1, z-1$; (v) $x, y, z + 1$; (vi) $-x + 1, -y + 3, -z$; (vii) $-x, -y + 2, -z + 1$; (viii) $x + 1, y, z$; (ix) $-x, -y + 2, -z + 2$; (x) $x-1$, y, $z + 1$; (xi) $x-1, y, z$

spectrum of $[Na_2(atpt)(H_2O)_5]\cdot H_2O$, the asymmetric absorption band $\nu_{as}(COO)^-$ at 1,573 cm^{-1} and the symmetric absorption band $\nu_s(COO)^-$ at 1,371 cm^{-1} appear, which indicates complete deprotonation of 2-aminoterephthalic acid. Another distinctive change observed in the FT-IR spectra of sodium complex in comparison with those of free acid refers to the shift in the positions and intensities of the absorption bands corresponding to the ν(N–H) and ν(O–H) vibrations. The broad and very strong absorption band with the maximum at 3,436 cm^{-1} is attributed to the overlapping ν(NH) and ν(OH) vibrations. The shift of the stretching asymmetric NH_2 vibrations to the lower frequencies by about 70 cm^{-1} is strongly connected with the presence of water molecules powerfully engaged in

Table 4 Experimental FT-IR wavenumbers for 2-aminoterephthalic acid and its sodium complex

Wavenumbers/cm^{-1}		Assignments
H_2atpt [28]	$[Na_2(atpt)(H_2O)_5]\cdot H_2O$	
3,508	3,436	$\nu_{as}NH_2$
3,393	3,393	$\nu_{as}NH_2$
	3,280	νOH (from H_2O)
3,055	3,060	$\nu C_{ar}H$
2,986		Overtone/combination
2,887		Overtone/combination
2,712		Overtone/combination
2,644		Overtone/combination
2,576	2,562	Overtone/combination
2,533	2,472	Overtone/combination
1,686	–	νC=O
1,625	1,621	$\nu C_{ar}C_{ar} + \delta$OH (from H_2O)[a]
1,593		$\rho NH_2 + \nu C_{ar}C_{ar}$
–	1,573	$\nu_{as}COO^-$
1,553	1,523	$\nu C_{ar}C_{ar} + \rho NH_2$
1,496	1,500	$\beta C_{ar}H + \nu C_{ar}C_{ar}$
1,453		$\nu C_{ar}C_{ar} + \nu C–NH_2$
1,419	1,416	$\nu C_{ar}C_{ar}$
–	1,371	$\nu_s COO^-$
1,316		βOH
1,233	1,239	$\beta C_{ar}H$
	1,152	$\beta C_{ar}H$
	1,130	$\beta C_{ar}H$
1,121		$\beta C_{ar}H + \beta$C–OH
915	957	$\beta C_{ar}C_{ar}C_{ar}$
882	899	$\gamma C_{ar}H$
831	834	$\gamma C_{ar}H$
782		γCCOO
753	773	Ring breathing
690		βOCOH
676	600	γCCC + γCCOO
588	505	βCCC
491	470	$\beta CC=O + \nu C_{ar}$–C
–	427	Na–O

[a] Only for sodium complex

hydrogen bond formation with amino group in this crystal structure. At the very low frequencies, a weak band of 427 cm^{-1} belongs to the stretching Na–O vibrations.

3.3 Thermal Study

The thermal stability of hexahydrated 2-aminoterephthalate with Na(I) was studied in air in the range 30–750 °C. The thermal behaviour of the synthesized complex was characterized on the basis of TG/DTG and DTA methods. The

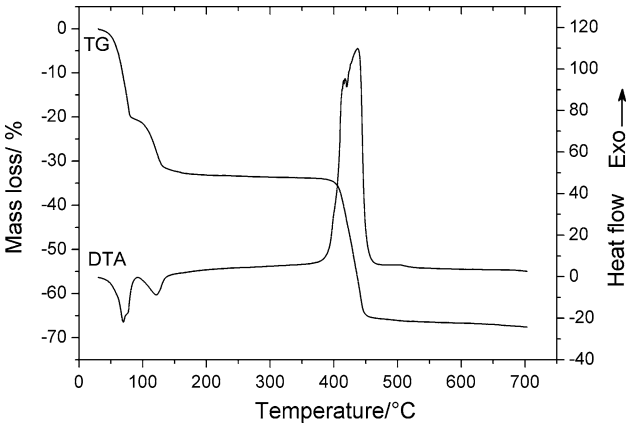

Fig. 3 TG and DTA curves of $[Na_2(atpt)(H_2O)_5].H_2O$ in air atmosphere

TG curve of the analysed complex shows three decomposition steps (Fig. 3). The decomposition process proceed in full in accordance with the following scheme:

$$[Na_2(atpt)(H_2O)_5]\cdot H_2O–4H_2O \rightarrow [Na_2(atpt)(H_2O)_2]–2H_2O \rightarrow Na_2(atpt) \rightarrow Na_2CO_3.$$

The first and second steps correspond to the loss of water molecules, whereas the last one is connected with degradation of organic part of the complex. The dehydration process begins at 30 °C and runs in two stages. In the first stage four water molecules per asymmetric unit are lost statistically (found 21.37 %; Calcd. 21.61 %). The second stage of dehydration process begins at 90 °C and goes off up to 205 °C. The TG curve in the mentioned temperature range shows loss of mass 11.13 % (Calcd. 10.81 %), which corresponds to the loss of two water molecules. The dehydration process is connected with the endothermic effect. The loss of all water molecules leads to creation of anhydrous compound, which is stable up to 370 °C. The anhydrous Na_2atpt is directly decomposed to sodium carbonate (Na_2CO_3), which is the final product of thermal decomposition. A weight loss of 67.88 % in the range of 370–470 °C is due to the removal of the atpt ligand per formula unit (Calcd. 68.19 %). The combustion of organic ligand is accompanied by a strong exothermic effect visible on the DTA curve.

3.4 TG–FT-IR Analysis

The decomposition process connected with release of gas products was carried out for $[Na_2(atpt)(H_2O)_5]\cdot H_2O$ to confirm the results obtained from thermal analysis. The FT-IR spectrum of gaseous products is presented in Fig. 4. As follows from Fig. 4 the dehydration process is reflected by the FT-IR spectra of gaseous decomposition at 50–200 °C. The characteristic valence and deformation vibration bands of water molecules appear in the wavenumber ranges of 3,950–3,500 cm^{-1} and 2,000–1,350 cm^{-1}, respectively. In

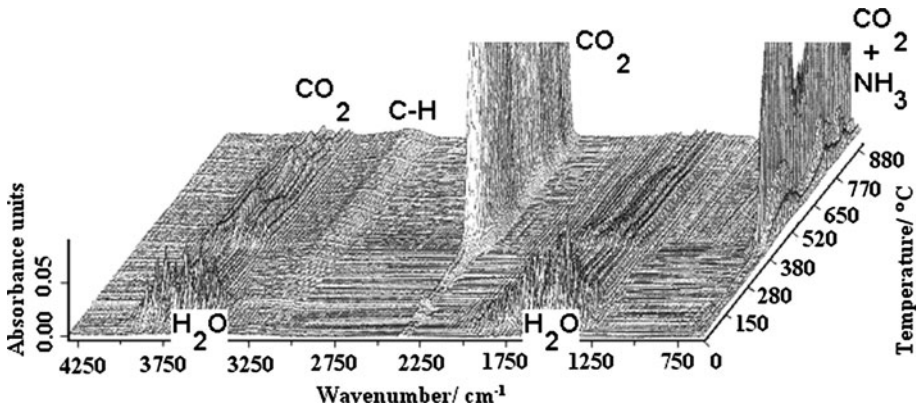

Fig. 4 FT-IR spectra of gaseous products of thermal decomposition of sodium 2-aminoterephthalate

the latter part of the dehydration process at 140 °C in the FT-IR spectra there appear weak bands in the range 2,900–2,250 cm^{-1} and 750–600 cm^{-1} characteristic of CO_2. This process is not observed on the TG curve, but slight changes are found on the DTG curve. Release of CO_2 is probably connected with partial decarboxylation and ends abruptly before dehydration is over. The last step of decomposition, which corresponds to the transformation of anhydrous compound into sodium carbonate is connected with the release of CO_2, CO, H_2O, NH_3 and hydrocarbons. The strong bands characteristic of CO_2 are observed on the FT-IR spectra at 380 °C. Within the range 390–570 °C the peaks characteristic of carbon monoxide (2,160 cm^{-1} and 2,095 cm^{-1}) are detected. At 440 °C the bands for NH_3 are observed in the range 750–1,200 cm^{-1} with the characteristic double-peak ones of the maxima at 966 and 931 cm^{-1}.

4 Conclusions

In summary, the novel sodium coordination polymer containing 2-aminoterephthalic ligand has been obtained by a conventional synthesis method in the form of a well-shaped single-crystals. The crystal structure analysis shows that the studied compound is a 2D coordination polymer with two crystallographically independent metal centers, which are coordinated via the tridentate chelate-bridged and monodentate carboxylate groups. The 2D layer structure is extended into the 3D supramolecular architecture by a net of strong O/N–H…O hydrogen bonds. The findings of supplementary techniques, such as FT-IR, TG–FT-IR and thermal analysis allowed to describe several additional properties, like the way and temperature range of dehydration process and decomposition of organic part of the complex (TG analysis) with determination of released gaseous products of decomposition (TG–FT-IR). Moreover, these supplementary findings also confirm the results obtained by the single-crystal X-ray diffraction technique, for the coordination with determination the functional groups participating in this process (FT-IR), the content of water molecules in the structure (FT-IR), the level of hydration (thermal analysis) and the participation of water molecules and amino group in creating the network of hydrogen bonds (FT-IR).

5 Supplementary material

CCDC-652105 contains the supplementary crystallographic data for this paper. These data can be obtained free of charge at www.ccdc.cam.ac.uk/conts/retrieving.html or from the Cambridge Crystallographic Data Centre (CCDC), 12 Union Road, Cambridge CB2 1EZ, UK; fax: (+44) 1223-336033; e-mail: deposit@ccdc.cam.ac.uk

References

1. H.X. Geng, Y.L. Feng, Y.Z. Lan, L.C. Kong, Struct. Chem. **20**, 877 (2009)
2. H.H. Zou, S.H. Zhang, Y. Xiao, C. Feng, Y.G. Wang, Struct. Chem. **22**, 135 (2011)
3. F.K. Wang, S.Y. Yang, R.B. Huang, L.S. Zheng, J. Chem. Crystallogr. **40**, 837 (2010)
4. K.O. Kongshaug, H. Fjellvåg, Polyhedron **26**, 5113 (2007)
5. Z. Rzączyńska, J. Sienkiewicz-Gromiuk, H. Głuchowska, J. Therm. Anal. Calorim. **101**, 213 (2010)
6. S.S. Kaye, A. Dailly, O.M. Yaghi, J.R. Long, J. Am. Chem. Soc. **129**, 14176 (2007)
7. H. Li, M. Eddaoudi, M. O'Keeffe, O.M. Yaghi, Nature **402**, 276 (1999)
8. G. Fèrey, C. Serre, C. Mellot-Draznieks, F. Millange, S. Surblé, J. Dutour, I. Margiolaki, Angew. Chem. Int. Ed. **43**, 6296 (2004)
9. K. Uemura, R. Matsuda, S. Kitagawa, J. Solid State Chem. **178**, 2420 (2005)
10. R. Łyszczek, Thermochim. Acta **509**, 120 (2010)
11. B. Moulton, M.J. Zawrotko, Chem. Rev. **101**, 1629 (2001)
12. G.R. Desiraju, Acc. Chem. Res. **29**, 441 (1996)
13. C. Sun, X. Zheng, L. Jin, J. Mol. Struct. **646**, 201 (2003)
14. C. Janiak, J. Chem Soc. Dalton Trans. 3885 (2000)

15. X.Y. Chen, B. Zhao, W. Shi, J. Xia, P. Cheng, D.Z. Liao, S.P. Yan, Z.H. Jiang, Chem. Mater. **17**, 2866 (2005)
16. C.B. Liu, X.J. Zheng, L.P. Jin, J. Chem. Crystallogr. **36**, 199 (2006)
17. X. Haitao, Z. Nengwu, J. Xianglin, Y. Ruyi, W. Yonggang, Y. Enyi, L. Zhengquan, J. Mol. Struct. **655**, 339 (2003)
18. C.B. Liu, C.Y. Sun, L.P. Jin, S.Z. Lu, New J. Chem. **28**, 1019 (2004)
19. M. Eddaoudi, J. Kim, N. Rosi, D. Vodak, J. Wachter, M. O'Keeffe, O.M. Yaghi, Science **295**, 469 (2002)
20. H.T. Xu, N.W. Zheng, X.L. Jin, R.Y. Yang, Z.Q. Li, J. Mol. Struct. **654**, 183 (2003)
21. A.L. Grzesiak, F.J. Uribe, N.W. Ockwig, O.M. Yaghi, A.J. Matzger, Angew. Chem. Int. Ed. **45**, 2553 (2006)
22. X. Haitao, Z. Nengwu, J. Xianglin, Y. Ruyi, L. Zhengquan, Chem. Lett. **31**, 350 (2002)
23. H.T. Xu, N.W. Zheng, X.L. Jin, R.Y. Yang, Z.Q. Li, J. Mol. Struct. **646**, 197 (2003)
24. Y. Wu, N. Zheng, R. Yang, H. Xu, E. Ye, J. Mol. Struct. **610**, 181 (2002)
25. G.M. Sheldrick, Acta Cryst. **A64**, 112 (2008)
26. C.M. Forsyth, P.M. Dean, D.R. MacFarlane, Acta Cryst. **C63**, m169 (2007)
27. F.H. Allen, Acta Cryst. **B58**, 380 (2002)
28. M. Karabacak, M. Cinar, Z. Unal, M. Kurt, J. Mol. Struct. **982**, 22 (2010)